CCFE
CULHAM CENTRE FOR FUSION ENERGY

UK Atomic Energy Authority

UKAEA-CCFE-PR(23)150

O. P. Bardsley, J. L. Baker

Decoupled magnetic control of spherical tokamak divertors via vacuum harmonic constraints

Decoupled magnetic control of spherical tokamak divertors via vacuum harmonic constraints

O. P. Bardsley, J. L. Baker

This is a preprint of a paper submitted for publication in
Plasma Physics and Controlled Fusion

Decoupled magnetic control of spherical tokamak divertors via vacuum harmonic constraints

Removed for double-anonymous peer review

Removed for double-anonymous peer review

E-mail: Removed for double-anonymous peer review

Abstract. Power exhaust is a critical challenge for spherical tokamak reactors, making the design, optimisation and control of advanced divertor configurations crucial. These tasks are greatly simplified if the poloidal magnetic fields in the core and divertor regions can be varied independently. We present a novel method which fixes the core plasma equilibrium whilst altering the divertor geometry, using vacuum spherical harmonic constraints. This has the advantage that it avoids iterative solution of the Grad-Shafranov equation, making it easy to use, rapid and reliable. By comparing a large number of MAST-U equilibrium reconstructions against their approximations using spherical harmonics, we show that a small number (~ 4) of harmonics is sufficient to closely reproduce the plasma boundary shape. When augmented with divertor geometry constraints, this method gives great flexibility in the creation of new exhaust configurations. We discuss how this approach would benefit applications in feed-forward scenario design, coilset optimisation, and real-time feedback control.

Keywords: Spherical Tokamaks, MHD equilibrium, Plasma Control, Divertor, Spherical Harmonics, Constrained Optimisation

Submitted to: *Plasma Phys. Control. Fusion*

1. Introduction

The spherical tokamak (ST) is attracting significant attention as a source of fusion energy [1–6] due to its potential for high plasma energy density and therefore reduced size and cost [7], made possible by recent advances in magnet technology [8]. However, the compactness of STs exacerbates the challenge of exhaust power handling, necessitating advanced divertor magnetic configurations to keep plasma facing components within material limits [2, 9]. This necessitates

- Testing candidate divertor magnetic geometries in present-day experimental devices (e.g. MAST-U);
- Designing poloidal field (PF) coil positions and currents capable of producing the scenarios required for a future power plant;
- Devising robust real-time control algorithms for divertor magnetic control in present and future devices.

A commonality here is the desire to keep a fixed core plasma shape (to ensure fair comparison, to match a given fixed-boundary solution, or to decouple shape and divertor controllers, respectively), whilst the divertor geometry is independently specified or controlled – a concept we henceforth refer to as just 'decoupling'. Because each PF coil affects both the core plasma and divertor magnetic geometries, controlling just the latter requires simultaneous adjustment of all the PF coil currents.

Existing inverse free-boundary equilibrium codes [10–15] generally solve this problem by minimising the distance of the plasma boundary from a set of control points, which may extend into the divertor region. The second-order non-linear Grad-Shafranov equation (GSE), which determines the plasma shape, is iteratively solved concurrently with the optimisation. This approach – which is compulsory for creating the core plasma shape – is well-understood, but when combining with divertor geometry optimisation it can be inflexible, challenging to formulate and slow to converge, particularly so when allowing coil positions to vary.

Here we demonstrate a novel decoupling approach which does not require iteration of the GSE. We make use of the fact that the core plasma shape is maintained as long as the vacuum magnetic field (i.e. that due to the PF coils) over the region of space it occupies remains unchanged, for a given internal current profile. Furthermore, for a ST the vacuum field is well-approximated by a spherical harmonic (SH) expansion truncated at just a few terms. Constraining these terms whilst the PF currents are varied provides a simple way to achieve decoupling without appeal to the GSE.

As complete, orthogonal solutions to the Laplace equation, SHs are widely employed in physics applications. For example, to model the effect of ferromagnetic walls on tokamak stability [16], in inertial confinement fusion for three-dimensional reconstructions [17] and compression models of radiation [18], for magnetic resonance imaging [19], and representing Earth's magnetic field [20, 21].

The objective of this paper is to describe and validate the method, and to this end we focus on the design and optimisation of divertor geometries for MAST-U, though it has potential for much wider applications in ST design and control. In section 2, we outline how SHs may be used to formulate simple constraints which replace the GSE in the context of a PF current optimisation problem. Our results (section 3) consist of validation and examples of divertor geometry generation on MAST-U. In section 4 we discuss how this approach may be exploited to meet the control needs of present and future STs.

2. Methods

We begin by recalling key aspects of tokamak equilibrium, then outline how vacuum SH constraints can be used to replace iteration of the GSE when modifying the divertor geometry for a particular core plasma.

In cylindrical polar co-ordinates $[R, \phi, Z]$, the poloidal magnetic flux density $\boldsymbol{B}_p(R, Z)$ for an axisymmetric tokamak equilibrium is found by integrating Ampère's law (i.e. the GSE),

$$\boldsymbol{e}_\phi \cdot \nabla^2 \left(A \boldsymbol{e}_\phi \right) = -\mu_0 j, \tag{1}$$

where $A(R, Z)\boldsymbol{e}_\phi$, the vector potential for $\boldsymbol{B}_p$, is related to the poloidal flux $\psi = AR$, $\boldsymbol{e}_\phi$ is the toroidal unit vector, $j(R, Z)$ is the toroidal current density, and μ_0 is the vacuum permeability.

The current density, and therefore A, has contributions due the plasma and PF coils, $j = j_{\text{pla}} + j_{\text{PF}}$. (For clarity we neglect passive structure currents here, but their contribution is similar to the PF coils.) j_{pla} is non-zero only in the region of space within the core plasma boundary Ω_{pla}, taking the form

$$j_{\text{pla}} = Rp' + \frac{ff'}{\mu_0 R}, \tag{2}$$

$p(\psi)$ being the plasma pressure and $f(\psi)$ the toroidal field function. j_{PF} can be represented by a set of δ-functions representing PF coil filaments.

If p' and ff' are known, the free-boundary equilibrium problem is to solve this system with the PF coil currents as inputs and the plasma boundary as an output, or vice versa, or some hybrid of the two. It is non-linear not only because (2) depends on ψ, but also

because $\Omega_{\rm pla}$ is unknown; this difficulty means solving the GSE necessitates an iterative method which is often time-consuming and numerically unstable.

Now suppose that this iteration has already been completed once, meaning $\Omega_{\rm pla}$ and the PF currents have been determined for some base case; this could be an experimental equilibrium reconstruction, or an inverse problem for the PF currents to give a desired core plasma shape. (Note this solution does not have to obey the constraints of – or even use the same coilset as – the following calculation.) We wish to alter the PF currents in some way that preserves this core plasma shape $\Omega_{\rm pla}$ and current distribution $j_{\rm pla}$, but gives us freedom to change the divertor magnetic geometry. It is key to realise that this wish will be satisfied if the field due to the PF coils (i.e. $A_{\rm PF}$) within the domain $\Omega_{\rm pla}$ does not change. The only way to keep $A_{\rm PF}|_{\Omega_{\rm pla}}$ strictly constant is to use exactly the same PF currents. However, the geometry of an ST lends itself naturally to representing $A_{\rm PF}|_{\Omega_{\rm pla}}$ as a series of SHs about the origin, and we assert that keeping just the first few terms of this series constant will in practice prove sufficient. So long as these coefficients are unchanged when choosing new PF currents, the core plasma shape will not change appreciably.

SH coefficients are easily related to the coilset geometry and PF currents. Introducing spherical polar co-ordinates $[r, \theta, \phi]$ so $R = r\sin\theta$ and $Z = r\cos\theta$, we have [22]

$$A_{\rm PF} = \sum_{\ell=1}^{\infty} A_{\rm PF}^{\ell} \left(\frac{r}{r_0}\right)^{\ell} \frac{P_\ell^1(\cos\theta)}{\sqrt{\ell(\ell+1)}}, \tag{3}$$

where $P_\ell^1(\cdot)$ is the associated Legendre polynomial of degree ℓ and order 1, and r_0 is a scaling length. For a set of toroidal filaments 'f' (making up a coil or whole coilset, say), the SH coefficients are given by

$$A_{\rm PF}^{\ell} = \sum_{f} \frac{\mu_0}{2} I_f \sin\theta_f \left(\frac{r_0}{r_f}\right)^{\ell} \frac{P_\ell^1(\cos\theta_f)}{\sqrt{\ell(\ell+1)}}, \tag{4}$$

with I_f being the current in each filament. We calculate the $A_{\rm PF}^{\ell}$ coefficients for the base case using (4), then require that the first $\ell_{\max}$ of them are fixed as the PF coil currents (and possibly positions) vary, again using (4). This gives $\ell_{\max}$ equality constraints (hereafter 'SH constraints') on the problem which entirely replace the GSE, and are linear in the free variables (I_f) for fixed coil positions.

It is important to note that (3) and (4) are only valid for locations within an imaginary sphere about the origin which does not contain any filaments, i.e. $r < \min(r_f)$. To use the method in its primitive form, this sphere must therefore contain the whole plasma volume, and hence only PF circuits with all $r_f > \max\left(r_{\partial\Omega_{\rm pla}}\right)$ may be free. This geometrical consideration limits the practicality to STs, and furthermore means that centre column PF currents must be held fixed, or otherwise compensated for in the optimisation (see section 3.3).

SH constraints can be fully exploited by combining with divertor geometry constraints. We limit discussion here to linear constraints, such as those on poloidal flux and field; for example, suppose we wish a point P to lie on the separatrix ('sep'), a desire we can write as

$$\psi|_P = \psi_{\rm PF}|_P + \psi_{\rm pla}|_P = \psi_{\rm sep}. \tag{5}$$

This gives a simple constraint on $\psi_{\rm PF}|_P$ which is merely a weighted sum of PF currents. This is only possible because the SH constraints ensure a fixed core plasma, meaning $\psi_{\rm pla}|_P$ and $\psi_{\rm sep}$ do not change. Although divertor geometry is usually formulated as a contribution to the objective function in such problems, there is now a natural distinction between hard plasma shape constraints (core and divertor) and the optimisation target.

Suppose this objective is quadratic, which encompasses a wide range of meaningful choices (see section 4.1). The least-squares problem for the free PF currents $\boldsymbol{x}$ is then

$$\begin{aligned} &\min_{\boldsymbol{x}} ||\mathsf{A}\boldsymbol{x} - \boldsymbol{b}||_2^2 \\ &\text{subject to } \mathsf{G}\boldsymbol{x} = \boldsymbol{c} \text{ and } \boldsymbol{x}_{\min} \le \boldsymbol{x} \le \boldsymbol{x}_{\max}, \end{aligned} \tag{6}$$

where we introduce A and $\boldsymbol{b}$ to encode the objective function, G and $\boldsymbol{c}$ to encode the linear SH and divertor constraints, and the current limits $\boldsymbol{x}_{\min|\max}$. The solution of this problem, ignoring bounds, amounts simply to the matrix multiplication

$$\boldsymbol{x} = \mathsf{N}(\mathsf{AN})^{+}\boldsymbol{b} + (\mathsf{I} - \mathsf{N}(\mathsf{AN})^{+}\mathsf{A})\mathsf{G}^{+}\boldsymbol{c} \tag{7}$$

where the columns of N span the nullspace of G, I is the identity matrix, and '+' denotes the pseudoinverse. To solve with bounds, we find values of $\boldsymbol{x}$ which are beyond limits, replace them with constraints at the limit, then solve (7) again.

3. Results

3.1. Verification of SH constraints

Our first task is to verify numerically that constraining a small number of vacuum SHs successfully preserves the core plasma shape. We take the EFIT++ reconstruction [23–25] of a MAST-U plasma and PF currents, recalculate the equilibrium using the free-boundary code Fiesta [26], then use (4) to calculate the SH coefficients due to the (non-centre-column) PF circuits. Keeping centre-column currents fixed, we replace the field due to the other PF circuits with the

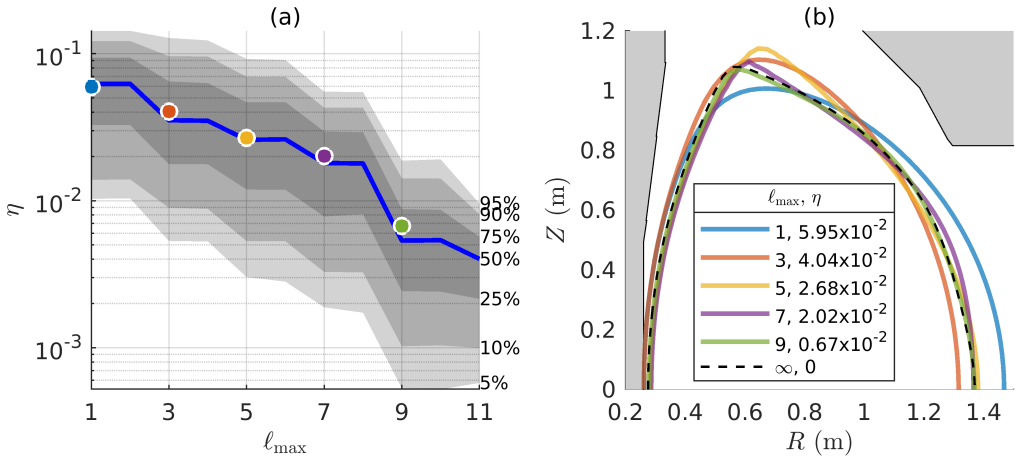

Figure 1. (a) Percentiles of the distribution of the fit metric η across 640 MAST-U equilibria as a function of the number of SHs used to approximate the vacuum field; (b) example boundary shapes and corresponding fit metrics for a single case (shot 44626 at 390ms), corresponding to markers in (a). Data citation: removed for double-anonymous peer review

series (3) truncated at degree $\ell_{\max}$, then recalculate the equilibrium once again. We assess the similarity between the two equilibria by evaluating a fit metric

$$\eta\left(\Omega^1_{\text{pla}}, \Omega^2_{\text{pla}}\right) := \frac{\text{XOR}\left(\Omega^1_{\text{pla}}, \Omega^2_{\text{pla}}\right)}{\Omega^1_{\text{pla}} + \Omega^2_{\text{pla}}}, \tag{8}$$

i.e. the area of the poloidal plane contained by only one plasma cross-section, divided by the sum of the areas — so a smaller η implies a better fit. This processes is repeated for 640 different plasmas (picked at random from MAST-U shots 43761-46799, times 0.1-1s, and with plasma current over 100kA) using $\ell_{\max} \in [1, 12]$, to give a statistical distribution for η as a function of $\ell_{\max}$.

Figure 1(a) shows how disparity between the base equilibrium and its approximation using SHs robustly decreases as $\ell_{\max}$ increases; an example case, which lies close to the median, is shown in Figure 1(b) to give intuition for interpretation of η. We see that a visual match to the plasma shape is obtained for $\eta \lesssim 10^{-2}$, and this is satisfied by the majority of cases when using 5 odd SHs ($\ell_{\max} = 9$). (Even SHs have up-down antisymmetric ψ, so are practically zero for the symmetric double-null plasmas of MAST-U.)

3.2. Combination with divertor constraints

Having verified robust efficacy of the method, we now exploit SH constraints to design ST divertor geometries and optimise the PF currents to produce them, taking MAST-U shot 45272 – a 750kA ELMy H-mode with conventional divertor leg – at 750ms as our base case. We solve the optimisation problem (6), minimising Ohmic dissipation in the PF coils, obeying relevant current limits, and constraining the first 4 odd SHs. In practice this proved sufficient to ensure $\eta \lesssim 10^{-2}$ whilst granting sufficient degrees of freedom. Additionally, a variety of divertor constraints related to magnetic flux and field are employed (as described in the caption of figure 2). The free-boundary equilibrium is recomputed after the optimisation of the PF currents to validate that η stays below our heuristic bound of 10^{-2}, and that divertor constraints are obeyed. This shows that wide range of divertor topologies can be generated in a way which is

- Intuitive: using a palette of divertor constraints to create exactly the desired geometry, and a single number $\ell_{\max}$ to determine the quality of core fit;
- Rapid: the problem (6) is a simple constrained least squares optimisation and its solution (7) is multiplication by a matrix with fewer elements than the number of PF coils squared;
- Robust: as shown in Figure 1 a good core fit is practically guaranteed for moderate $\ell_{\max}$, without requiring the expertise to design boundary control points.

3.3. Centre column circuit compensation

As mentioned in section 2, the expression (4) cannot be applied directly to PF coils within the imaginary sphere which just encloses the plasma. However, this is resolved by determining a weighted sum of SHs which cancel out the field (though not flux) due to these circuits over Ω_{pla}, and using (minus) these weights in place of (4). Figure 3 shows this approach applied to the MAST-U central solenoid, showing that SHs are a natural, coilset-independent way to compensate for its stray field.

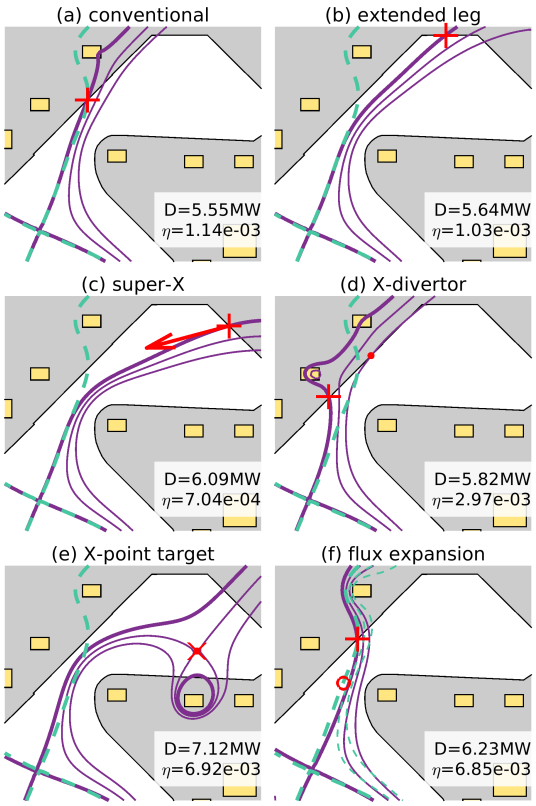

Figure 2. Examples of divertor geometry design and optimisation. Dashed turquoise lines are the base case and solid purple lines the optimised equilibria; thick lines are the plasma separatrix and thin lines at normalised flux of 1.05 and 1.1. Red symbols denote divertor constraints: crosses (+) are separatrix constraints, the arrow in (c) is a poloidal field direction constraint, dots are normalised flux constraints (1.1 in (d), 1.05 in (e)), the × in (e) is an X-point constraint, and the circle in (f) is a poloidal field constraint to 75% of the base case value. The Ohmic dissipation D (which is 6.39MW in the base case) and core plasma fit metric η are shown.

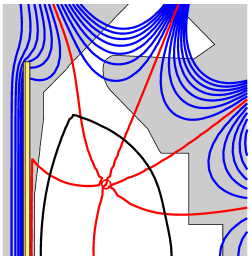

Figure 3. Contours of flux (blue/red) due to central solenoid (yellow), plus the four odd SHs which give $\boldsymbol{B}_p = \nabla \boldsymbol{B}_p = \mathbf{0}$ at the red circle. The boundary of shot 45272 at 750ms is in black.

4. Discussion and further work

We have demonstrated intuitive, optimal core-divertor decoupling is possible using SH constraints, making them a powerful tool to address a variety of control challenges for present and future STs. We refer back to the control needs identified in our introduction.

4.1. Testing novel divertor geometries

We have shown (Figure 2) that calculation of feed-forward PF currents for a desired exhaust solution is straightforward using SH constraints. This robust tool requires minimal expertise in free-boundary equilibria, yet is fast and flexible. The optimisation formulation means it can reveal when the imposed constraints are impossible to realise, and reduces chances of losing shots to coil current limit violations. As the divertor geometry is constrained (rather than optimised towards), it can be specified precisely, e.g. for systematic parameter scans. Note the minimisation objective is quite generic; we have chosen Ohmic dissipation, but one could also consider stored magnetic energy, change in currents from the base case, closeness to some desired divertor parameter, or inter-coil forces, to give some further examples. (Note generalised objective functions and non-linear extra constraints are also feasible.) Finally we remark that SH are a natural way to transplant scenarios between devices, since they represent the core chamber vacuum field without reference to the coilset.

4.2. Reactor coilset and scenario design

For feed-forward generation of flat-top scenarios, SHs offer much the same advantages as for present-day devices. Furthermore, they can aid the design of transient control scenarios (e.g. inductive ramp and LH transitions) by including the passive structure contribution to the SHs and solving an inverse problem similar to [27] with desired waveforms for the SHs.

Additionally, optimisation of PF coil positions and currents simultaneously could be accelerated and stabilised by replacing the GSE iteration with SH constraints. The problem is still non-linear, through the dependence of (4) on r_f and θ_f, but the constraints are differentiable in these variables, making for a relatively straightforward problem. Work is ongoing to implement this approach in BLUEMIRA [10, 28].

Furthermore, we note that the basic principle could also apply to conventional aspect ratio devices, by expanding the vacuum field using toroidal harmonics [29] rather than SHs.

4.3. Feedback control

Although we have not explored this in detail here, the speed and robustness of this method lends itself to real-time control applications. For example, it is trivial to design plasma-independent control vectors (i.e. sets of PF current weights, or "virtual circuits (VCs)") which make no change to the first $\ell_{\max}$ SHs – and therefore

negligibly change the core plasma shape – but do make a maximal change to some divertor property. This could be applied to feedback control on the strike point location, including sweeping, or for detachment control using flux expansion [30], for example. Similar "null VCs" could also be used to steer away from current limits without compromising the core plasma shape.

Going a step further, plasma shape and current control could also be managed through SHs; rather than allocating specific circuits, or even VCs [31], to control shape parameters, one could allocate a set of SHs. Adding these to any feed-forward SHs, plus the necessary SHs to cancel out the solenoid field (see Section 3.3), gives a real-time request for $\boldsymbol{c}$ which is converted into an optimised set of currents $\boldsymbol{x}$ by the matrix multiplication (7). In this way, feedback control of the plasma shape is regularised by actuating only with the low-ℓ SHs – we have shown high-ℓ terms have little influence – and following this, the best PF currents to produce these SHs are determined.

Full exploitation of SHs for ST magnetic control will be reported in future work.

Acknowledgements

Removed for double-anonymous peer review.

References

1. Windridge, M. Smaller and quicker with spherical tokamaks and high-temperature superconductors. *Philosophical transactions. Series A, Mathematical, physical, and engineering sciences* **377,** 20170438. ISSN: 1364-503X. https://www.ncbi.nlm.nih.gov/pmc/articles/PMC6365856/ (2022) (Mar. 2019).
2. Menard, J. E. *et al.* Fusion nuclear science facilities and pilot plants based on the spherical tokamak. en. *Nuclear Fusion* **56.** Publisher: IOP Publishing, 106023. ISSN: 0029-5515. https://dx.doi.org/10.1088/0029-5515/56/10/106023 (2022) (Aug. 2016).
3. Wilson, H. *et al.* en. in *Commercialising Fusion Energy: How small businesses are transforming big science* (IOP Publishing, Dec. 2020). http://iopscience.iop.org/book/edit/978-0-7503-2719-0/chapter/bk978-0-7503-2719-0ch8 (2022).
4. Morris, W. *et al.* MAST Upgrade Divertor Facility: A Test Bed for Novel Divertor Solutions. *IEEE Transactions on Plasma Science* **46.** Conference Name: IEEE Transactions on Plasma Science, 1217–1226. ISSN: 1939-9375 (May 2018).
5. Kurskiev, G. S. *et al.* Energy confinement in the spherical tokamak Globus-M2 with a toroidal magnetic field reaching 0.8 T. en. *Nuclear Fusion* **62.** Publisher: IOP Publishing, 016011. ISSN: 0029-5515. https://dx.doi.org/10.1088/1741-4326/ac38c9 (2023) (Dec. 2021).
6. Creely, A. J. *et al.* Overview of the SPARC tokamak. en. *Journal of Plasma Physics* **86.** Publisher: Cambridge University Press, 865860502. ISSN: 0022-3778, 1469-7807. https://www.cambridge.org/core/journals/journal-of-plasma-physics/article/overview-of-the-sparc-tokamak/DD3C44ECD26F5EACC554811764EF9FF0 (2022) (Oct. 2020).
7. Buxton, P. F., Connor, J. W., Costley, A. E., Gryaznevich, M. P. & McNamara, S. On the energy confinement time in spherical tokamaks: implications for the design of pilot plants and fusion reactors. en. *Plasma Physics and Controlled Fusion* **61.** Publisher: IOP Publishing, 035006. ISSN: 0741-3335. https://dx.doi.org/10.1088/1361-6587/aaf7e5 (2023) (Jan. 2019).
8. Bruzzone, P. *et al.* High temperature superconductors for fusion magnets. en. *Nuclear Fusion* **58.** Publisher: IOP Publishing, 103001. ISSN: 0029-5515. https://dx.doi.org/10.1088/1741-4326/aad835 (2023) (Aug. 2018).
9. Sykes, A. *et al.* Compact fusion energy based on the spherical tokamak. en. *Nuclear Fusion* **58,** 016039. ISSN: 0029-5515, 1741-4326. https://iopscience.iop.org/article/10.1088/1741-4326/aa8c8d (2022) (Jan. 2018).
10. Coleman, M. & McIntosh, S. BLUEPRINT: A novel approach to fusion reactor design. en. *Fusion Engineering and Design* **139,** 26–38. ISSN: 0920-3796. https://www.sciencedirect.com/science/article/pii/S0920379618308019 (2022) (Feb. 2019).
11. Faugeras, B. An overview of the numerical methods for tokamak plasma equilibrium computation implemented in the NICE code. en. *Fusion Engineering and Design* **160,** 112020. ISSN: 0920-3796. https://www.sciencedirect.com/science/article/pii/S0920379620305688 (2023) (Nov. 2020).
12. Hofmann, F. FBT - a free-boundary tokamak equilibrium code for highly elongated and shaped plasmas. en. *Computer Physics Communications* **48,** 207–221. ISSN: 0010-4655. https://www.sciencedirect.com/science/article/pii/0010465588900410 (2023) (Feb. 1988).

13. Welander, A., Olofsson, E., Sammuli, B., Walker, M. L. & Xiao, B. Closed-loop simulation with Grad-Shafranov equilibrium evolution for plasma control system development. en. *Fusion Engineering and Design. SI:SOFT-30* **146,** 2361–2365. ISSN: 0920-3796. https://www.sciencedirect.com/science/article/pii/S0920379619305241 (2023) (Sept. 2019).
14. Ambrosino, G. *et al.* XSC plasma control: Tool development for the session leader. en. *Fusion Engineering and Design. Proceedings of the 23rd Symposium of Fusion Technology* **74,** 521–525. ISSN: 0920-3796. https://www.sciencedirect.com/science/article/pii/S0920379605001146 (2023) (Nov. 2005).
15. Khayrutdinov, R. R. & Lukash, V. E. Studies of Plasma Equilibrium and Transport in a Tokamak Fusion Device with the Inverse-Variable Technique. en. *Journal of Computational Physics* **109,** 193–201. ISSN: 0021-9991. https://www.sciencedirect.com/science/article/pii/S0021999183712118 (2023) (Dec. 1993).
16. Bardsley, O. P. & Hender, T. C. On the axisymmetric stability of tokamaks with ferromagnetic walls. *Physics of Plasmas* **27.** Publisher: American Institute of Physics, 102508. ISSN: 1070-664X. https://aip.scitation.org/doi/full/10.1063/5.0018747 (2022) (Oct. 2020).
17. Volegov, P. L. *et al.* Three-dimensional reconstruction of neutron, gamma-ray, and x-ray sources using spherical harmonic decomposition. *Journal of Applied Physics* **122.** Publisher: American Institute of Physics, 175901. ISSN: 0021-8979. https://aip.scitation.org/doi/full/10.1063/1.4986652 (2023) (Nov. 2017).
18. Li, H., Liang, G. & Huang, Y. An efficient radiation analysis approach through compressive model for laser driven inertial confinement fusion. en. *Computer Physics Communications* **259,** 107644. ISSN: 0010-4655. https://www.sciencedirect.com/science/article/pii/S001046552030312X (2022) (Feb. 2021).
19. Li, F. X. *et al.* An analytical approach towards passive ferromagnetic shimming design for a high-resolution NMR magnet. en. *Superconductor Science and Technology* **28.** Publisher: IOP Publishing, 075006. ISSN: 0953-2048. https://dx.doi.org/10.1088/0953-2048/28/7/075006 (2022) (May 2015).
20. Thébault, E., Hulot, G., Langlais, B. & Vigneron, P. A Spherical Harmonic Model of Earth's Lithospheric Magnetic Field up to Degree 1050. en. *Geophysical Research Letters* **48.** _eprint: https://onlinelibrary.wiley.com/doi/pdf/10.1029/2021GL095147, e2021GL095147. ISSN: 1944-8007. https://onlinelibrary.wiley.com/doi/abs/10.1029/2021GL095147 (2022) (2021).
21. Finlay, C. C. *et al.* The CHAOS-7 geomagnetic field model and observed changes in the South Atlantic Anomaly. *Earth, Planets and Space* **72,** 156. ISSN: 1880-5981. https://doi.org/10.1186/s40623-020-01252-9 (2023) (Oct. 2020).
22. Jackson, J. D. *Classical electrodynamics; 3nd edition* https://www.wiley.com/en-us/Classical+Electrodynamics%2C+3rd+Edition-p-9780471309321 (Wiley, 1998).
23. Lao, L. L., John, H. S., Stambaugh, R. D., Kellman, A. G. & Pfeiffer, W. Reconstruction of current profile parameters and plasma shapes in tokamaks. en. *Nuclear Fusion* **25,** 1611. ISSN: 0029-5515. https://dx.doi.org/10.1088/0029-5515/25/11/007 (2023) (Nov. 1985).
24. MAST Upgrade team *et al.* First MAST-U Equilibrium Reconstructions using the EFIT++ code: 48th European Physical Society Conference on Plasma Physics, EPS 2022. *48th EPS Conference on Plasma Physics 27 June - 1 July 2022. Europhysics conference abstracts* Publisher: European Physical Society (EPS). http://www.scopus.com/inward/record.url?scp=85145838022&partnerID=8YFLogxK (2023) (2022).
25. Berkery, J. W. *et al.* Kinetic equilibrium reconstructions of plasmas in the MAST database and preparation for reconstruction of the first plasmas in MAST upgrade. en. *Plasma Physics and Controlled Fusion* **63.** Publisher: IOP Publishing, 055014. ISSN: 0741-3335. https://dx.doi.org/10.1088/1361-6587/abf230 (2023) (Apr. 2021).
26. Cunningham, G. High performance plasma vertical position control system for upgraded MAST. en. *Fusion Engineering and Design* **88,** 3238–3247. ISSN: 0920-3796. https://www.sciencedirect.com/science/article/pii/S0920379613006753 (2023) (Dec. 2013).
27. Di Grazia, L. E. & Mattei, M. A numerical tool to optimize voltage waveforms for plasma breakdown and early ramp-up in the presence of constraints. en. *Fusion Engineering and Design* **176,** 113027. ISSN: 0920-3796. https://www.sciencedirect.com/science/article/pii/S0920379622000278 (2023) (Mar. 2022).
28. Franza, F. *et al.* MIRA: a multi-physics approach to designing a fusion power plant. en. *Nuclear Fusion* **62.** Publisher: IOP Publishing, 076042. ISSN: 0029-5515. https://dx.doi.org/10.1088/1741-4326/ac6433 (2023) (June 2022).

29. Alladio, F. & Crisanti, F. Analysis of MHD equilibria by toroidal multipolar expansions. en. *Nuclear Fusion* **26,** 1143. ISSN: 0029-5515. https://dx.doi.org/10.1088/0029-5515/26/9/002 (2023) (Sept. 1986).

30. Anand, H. *et al.* Plasma flux expansion control on the DIII-D tokamak. en. *Plasma Physics and Controlled Fusion* **63.** Publisher: IOP Publishing, 015006. ISSN: 0741-3335. https://dx.doi.org/10.1088/1361-6587/abc457 (2023) (Nov. 2020).

31. McArdle, G., Pangione, L. & Kochan, M. The MAST Upgrade plasma control system. en. *Fusion Engineering and Design* **159,** 111764. ISSN: 0920-3796. https://www.sciencedirect.com/science/article/pii/S0920379620303124 (2022) (Oct. 2020).